Local and Remote Impacts of Atmospheric Cloud Radiative Effects Onto the Eddy-Driven Jet

O. Watt-Meyer[1] (iD) and D. M. W. Frierson[1] (iD)

[1]Department of Atmospheric Sciences, University of Washington, Seattle, WA, USA

Abstract This study examines the cause of the spread of extratropical circulation responses to the inclusion of atmospheric cloud radiative effects (ACRE) across atmospheric general circulation models. The ensemble of Clouds On-Off Klimate Intercomparison Experiment aquaplanet simulations shows that these responses include both equatorward and poleward shifts of the eddy-driven jet of varying magnitudes. These disparate extratropical responses occur despite the relatively consistent response in the tropics: a heating in the upper troposphere, which leads to a strengthening of the Hadley cell. It is argued that the eddy-driven jet response is a competition between two effects: the local influence of clouds driving shifts of the jet through meridional gradients in ACRE and the remote impact of a strengthened Hadley cell causing an equatorward shift of the eddy-driven jet. Simulations in which cloud radiative effects are separately turned on in the tropics and extratropics demonstrate this explicitly.

1. Introduction

It is being increasingly recognized that there are strong two-way interactions between cloud radiative effects and the large-scale atmospheric circulation (Bony et al., 2015; Ceppi & Hartmann, 2015). In general circulation models, cloud radiative effects have been shown to have significant impacts on the mean circulation in the tropics, including acting to strengthen the Hadley cell and subtropical jets and modify the position of the Intertropical Convergence Zone (Harrop & Hartmann, 2016; Li et al., 2015; Slingo & Slingo, 1988, 1991). Clouds also modify the variability of the tropics, from intraseasonal timescales associated with the Madden-Julian Oscillation (Crueger & Stevens, 2015) to the interannual timescales of the El Niño–Southern Oscillation (Rädel et al., 2016). Cloud radiative effects are also connected with extratropical annular mode variability, as shown both in observations (Li & Thompson, 2016; Li et al., 2014) and in models (Grise & Medeiros, 2016; Grise & Polvani, 2014), and with Hadley cell extent (Tselioudis et al., 2016). Biases in the surface shortwave cloud radiative forcing have been shown to be connected to biases in the climatological position of the Southern Hemisphere jet latitude (Ceppi et al., 2012) and the double-Intertropical Convergence Zone (ITCZ) problem (Hwang & Frierson, 2013) in coupled climate models. Clouds also play a role in the dynamical response to external forcing such as increased greenhouse gases. For example, cloud radiative effects have been shown to be responsible for half or more of the poleward shift of the eddy-driven jet in response to either uniformly increased sea surface temperatures (Voigt & Shaw, 2015) or increased CO_2 concentrations (Ceppi & Hartmann, 2016) in specified-sea surface temperature (SST) and slab-ocean aquaplanet simulations, respectively.

The focus of this study is on understanding the impact of atmospheric cloud radiative effects onto the climatological position of the eddy-driven jet in atmospheric general circulation models (GCMs). The study will examine simulations with specified SSTs and hence focuses on the impacts of cloud heating and cooling within the atmosphere, not the impacts of clouds onto the surface energy budget. The eddy-driven jet is a region of strong westerly zonal wind that extends through the depth of the troposphere and exists due to the convergence of angular momentum by eddies (that is, the cyclones and anticyclones generated by baroclinic instability) into a region of maximum baroclinicity. The position of the eddy-driven jet is of fundamental importance for surface climate, as it is related to the meridional maximum in cyclone activity and extratropical precipitation (see review, Shaw et al., 2016). Furthermore, the latitude of the eddy-driven jet is connected to its timescale of variability (Barnes & Hartmann, 2010), which the fluctuation-dissipation theorem suggests is related to the sensitivity of the jet to external forcing such as increased greenhouse gas concentrations (Kidston & Gerber, 2010; but see also Simpson & Polvani, 2016). Modern climate models are also known to have significant equatorward biases in the position of the eddy-driven jet in the Southern
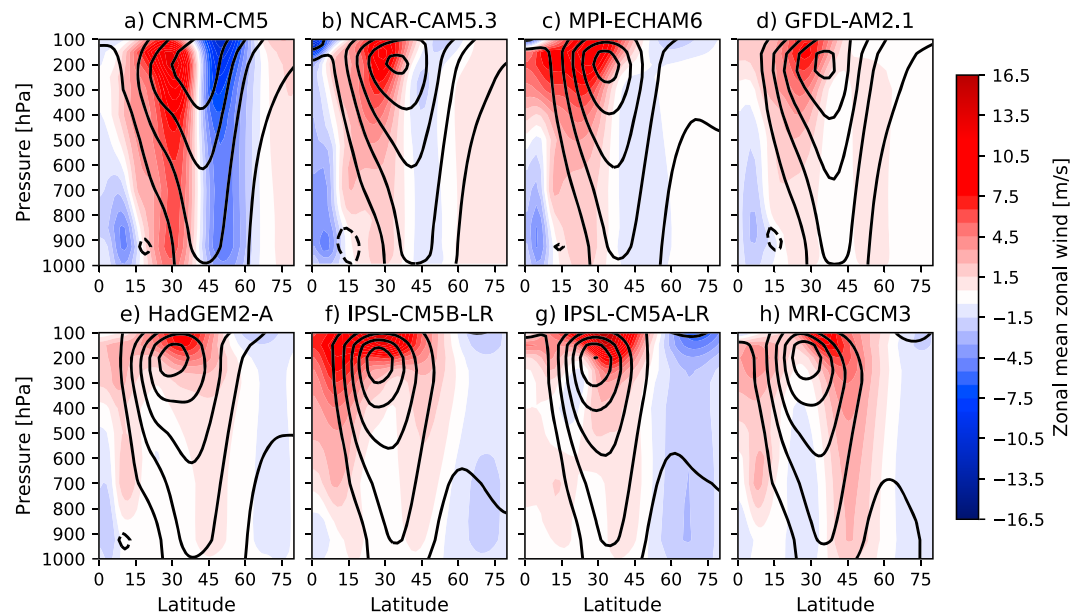
Figure 1. The zonal-mean zonal wind in the clouds-off experiment (black contours, 10 m/s intervals) and the difference in wind between the clouds-on and clouds-off experiment (shaded contours) for each model in the COOKIE ensemble.

Hemisphere compared to reanalysis (Bracegirdle et al., 2013). For these reasons, it is important to understand what factors determine the position of the eddy-driven jet in atmospheric models. One such factor is the impact of cloud radiative effects onto the jet.

Despite many studies focused on the connections between cloud radiative effects and dynamical processes in the atmosphere, there is no consensus on the impact of clouds onto the climatological position of the eddy-driven jet. Figure 1 shows the response of the zonal-mean zonal wind to the inclusion of atmospheric cloud radiative effects in eight different GCMs (details on the simulations are given in section 2). It is evident that the response of the eddy-driven jet widely varies across models, including a strong equatorward shift (CNRM-CM5; Figure 1a), a poleward shift (MRI-CGCM3; Figure 1h), and a broadening of the jet (GFDL-AM2.1; Figure 1d). The fact that cloud radiative effects have such disparate impacts on the climatological position of the eddy-driven jet across models suggest that the degree to which cloud radiative effects amplify the poleward shift of the jet under global warming (Ceppi & Hartmann, 2016; Voigt & Shaw, 2015, 2016) may be model dependent. The goal of this study is to understand the spread of responses of the eddy-driven jet to cloud radiative effects across models. Briefly, it is found that the response can be explained as a result of two competing effects: tropical cloud radiative effects drive a strengthening of the Hadley cell and an equatorward shifted eddy-driven jet, while extratropical cloud radiative effects impact local baroclinicity in such a way as to shift the jet poleward.

2. Data and Methods

This study uses model output from the Clouds On-Off Klimate Intercomparison Experiment (COOKIE; Stevens et al., 2012), in which simulations are performed with cloud radiative effects turned off ("clouds-off"). That is, the radiative transfer scheme in each model is made to ignore the presence of clouds. These experiments are then compared to control simulations that include cloud radiative effects ("clouds-on"). This experimental procedure, pioneered by Slingo and Slingo (1988), is practical for explicitly identifying the impacts of atmospheric cloud radiative effects onto the modeled circulation. The focus here is on specified-SST aquaplanet simulations, which use the QOBS SST profile and otherwise follow the specifications of the Aqua-Planet Experiment (Neale & Hoskins, 2000). Using specified-SST aquaplanet experiments eliminates concerns about oceans or land surface warming unrealistically in clouds-off simulations, due to the negative net cloud radiative forcing onto the climate (e.g., Ramanathan et al., 1989). It also simplifies analysis and interpretation due

to the zonal symmetry of the boundary conditions. The COOKIE ensemble includes five models: CNRM (Voldoire et al., 2013), MPI (Stevens et al., 2013), HadGEM (Collins et al., 2008), IPSL (Dufresne et al., 2013), and MRI (Yukimoto et al., 2012). The IPSL model is run with two different physics packages, which are referred to as IPSL-A and IPSL-B, respectively (Hourdin, Foujols, et al., 2013; Hourdin, Grandpeix, et al., 2013). Each model is run for 5 years, with no seasonal cycle and perpetual equinoctial solar insolation. In addition to the standard set of COOKIE simulations, additional experiments are performed for this study with the GFDL-AM2.1 (Anderson et al., 2004) and the NCAR-CAM5.3 (Medeiros et al., 2016) models. Standard clouds-on and clouds-off simulations are performed, with the same specifications as the COOKIE ensemble. The GFDL-AM2.1 experiments are run for 60 years each, while the NCAR-CAM5.3 experiments are run for 5 years each. As well, experiments are performed with the GFDL and NCAR models in which cloud radiative effects are only turned on or off in certain latitude bands. Two additional experiments with the GFDL model only turn on cloud radiative effects for the longwave and shortwave bands, respectively. The details of these experiments are described in the supporting information. Because of the hemispheric symmetry of the simulations, Northern and Southern Hemispheres are averaged, but it has been verified that there is no qualitative change in the results if only the Northern or Southern Hemispheres are used.

The position of the eddy-driven jet is quantified as the latitude of the maximum zonal-mean zonal wind at 850 hPa (844 hPa and 860 hPa for the GFDL AM2.1 and NCAR-CAM5.3 simulations, respectively). The latitude is computed by fitting a quadratic polynomial to the grid point of maximum wind and two points on either side (Simpson & Polvani, 2016) and is denoted ϕ_{on} and ϕ_{off} for the clouds-on and clouds-off experiments, respectively. The strength of the Hadley cell is measured as the maximum of the meridional mass stream function and is denoted ψ_{on} and ψ_{off} for the clouds-on and clouds-off experiments, respectively. The difference in the eddy-driven jet latitude and the Hadley cell strength between the clouds-off and the cloud-on simulations are denoted $\Delta\phi = \phi_{on} - \phi_{off}$ and $\Delta\psi = \psi_{on} - \psi_{off}$, respectively. To measure the impact of cloud radiative effects onto the meridional temperature gradient of the atmosphere, the net atmospheric cloud radiative effect (ACRE) is computed. Specifically,

$$ACRE = swup\_sfc_{cld} - swup\_toa_{cld} - swdn\_sfc_{cld} - lwdn\_sfc_{cld} - lwup\_toa_{cld} \qquad (1)$$

where the "cld" subscript represents the difference between total and clear-sky radiative fluxes, that is, $swup\_sfc_{cld} = swup\_sfc - swup\_sfc_{clr}$. This quantity is computed for all of the clouds-on experiments and is also computed for clouds-off experiments for the models that output the necessary data (the ACRE is only computed for diagnostic purposes in the clouds-off experiments; it is not actually imposed in the model simulations).

Following the Eady growth rate assumption, the meridional position of maximum eddy growth, and thus the position of the eddy-driven jet, tends to be collocated with the maximum absolute temperature gradient (e.g., Lindzen & Farrell, 1980). To quantify the impact of ACRE onto the temperature gradient of the atmosphere near the jet position, we compute a measure of the second derivative of the ACRE at the latitude of the eddy-driven jet:

$$ACRE_{\phi\phi} = \overline{ACRE}(\phi_{off} - \alpha) - 2 \cdot \overline{ACRE}(\phi_{off}) + \overline{ACRE}(\phi_{off} + \alpha) \qquad (2)$$

where

$$\overline{ACRE}(\phi') = \underset{|\phi-\phi'|<\frac{\alpha}{2}}{mean} [ACRE(\phi)]. \qquad (3)$$

In equations (2) and (3), α is a parameter which represents the meridional extent over which the ACRE is smoothed before the second derivative is calculated. A range of values of α were tested, and for the results shown in the next section, $\alpha = 5°$ will be used. In the Northern Hemisphere, the climatological meridional gradient of temperature is negative. Thus, when $ACRE_{\phi\phi}$ is negative, cloud radiative effects act to increase the absolute value of the gradient poleward of the clouds-off jet position and/or decrease it equatorward of the clouds-off jet position. This indicates that local cloud radiative effects will act to shift the jet poleward when $ACRE_{\phi\phi}$ is negative, and equatorward when it is positive.

Text

Table 1
Eddy-Driven Jet Latitudes, Hadley Cell Strengths, and ACRE$_{\phi\phi}$ Across All Models

Model	ϕ_{off} (°)	$\Delta\phi$ (° poleward)	ψ_{off} (10^9 kg/s)	$\Delta\psi$ (10^9 kg/s)	ACRE$_{\phi\phi}$ (W/m^2)
CNRM-CM5.1	43.4	−4.70	106.1	53.3	−2.20
NCAR-CAM5.3	42.3	−1.21	135.6	45.0	−2.61
MPI-ECHAM6	38.5	−1.16	180.0	62.5	−2.65
GFDL-AM2.1	39.7	−0.03	160.4	38.7	−2.91
HadGEM2-A	39.1	0.49	219.6	56.6	−5.80
IPSL-CM5B-LR	34.3	0.65	195.5	12.0	−2.39
IPSL-CM5A-LR	34.7	0.85	172.2	−20.5	−4.98
MRI-CGCM3	35.2	1.88	222.4	15.5	−4.46

Note. In this table and in all figures, the models are sorted in order of increasing $\Delta\phi$.

Across the model simulations examined, there is a strong connection ($r = 0.89$) between the Hadley cell edge, as diagnosed by the first zero crossing of the 500 hPa mass stream function, and the eddy-driven jet latitude (e.g., Kang & Polvani, 2011). Thus, the explanations for the shift of the eddy-driven jet equivalently apply to explain changes in the width of the Hadley cell.

3. Results

The response of the position of the eddy-driven jet to the inclusion of cloud radiative effects varies widely across models both in magnitude and sign (Figure 1). In some models, the jet shifts equatorward (CNRM-CM5, MPI-ECHAM6, and NCAR-CAM5.3), in another there is a clear poleward shift (MRI-CGCM3) and in another there is no change in position, but a broadening of the jet (GFDL-AM2.1). Table 1 lists the eddy-driven jet shift for each model. This spread of responses occurs despite a relatively consistent response across the models of a strengthened Hadley cell and equatorward contracted ITCZ (Figure S2 and see Harrop & Hartmann, 2016), and an accelerated subtropical jet. The strengthened Hadley circulation can be understood as a response to the cloud radiative heating in the tropical upper troposphere (Figure S3). The heating has a strong meridional gradient, which the Hadley cell responds to by accelerating in order to export more energy from the tropics. This directly leads to a strengthening of the subtropical jet by the transport of westerly angular momentum. The strength of the subtropical jet is known to be related to the position of the eddy-driven jet, with a stronger subtropical jet being associated with an equatorward shifted eddy-driven jet (Ceppi et al., 2013; Lee & Kim, 2003). There are multiple theories to explain this connection, including the possibility of stronger baroclinicity on the poleward flank of the subtropical jet when it is strong (Brayshaw et al., 2008; Lee & Kim, 2003) or because eddies generated in the midlatitudes are able to propagate further equatorward with a stronger subtropical jet (Barnes & Hartmann, 2011; Ceppi et al., 2013).

However, despite the increase in the strength of the Hadley cell in nearly all of the eight models (Figure S2 and Table 1), there is only a clear equatorward shift of the eddy-driven jet in three models (CNRM-CM5, NCAR-CAM5.3, and MPI-ECHAM6, Figures 1a–1c). This suggests that cloud radiative effects must be affecting the position of the jet through a mechanism beyond their impact on the strength of the Hadley cell. In order to explore this possibility, additional simulations were performed with the GFDL-AM2.1 and NCAR-CAM5.3 models in which cloud radiative effects were only turned on in certain latitude bands (see supporting information). Figure 2 shows the zonal wind response to cloud radiative effects imposed only in the tropics (equatorward of 30°; second column of Figure 2) and only in the extratropics (poleward of 30°; third column of Figure 2). In both models, there are opposing impacts from the cloud radiative effects in each region: tropical clouds drive a strong equatorward shift of the jet, consistent with the strengthening of the Hadley cell (Figure S4), while clouds in the extratropics shift the eddy-driven jet poleward. When including cloud radiative effects at all latitudes, these effects nearly exactly cancel at 850 hPa for the GFDL-AM2.1 model, while the tropical response is slightly stronger for the NCAR-CAM5.3 model (Figure 2, fourth column). This results in no shift of the eddy-driven jet for the GFDL-AM2.1 model, and a moderate equatorward shift for the NCAR-CAM5.3 model for the response to all clouds. These experiments suggest that cloud radiative effects in the tropics and extratropics act as competing influences on the position of the eddy-driven jet.
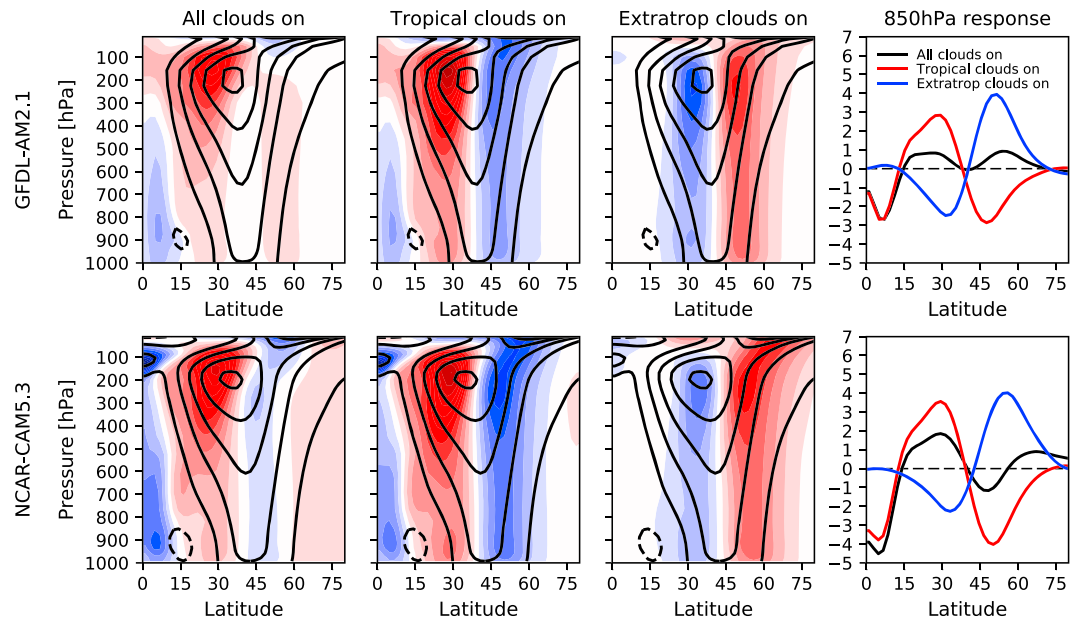
Figure 2. The zonal-mean zonal wind in the (top row) GFDL-AM2.1 and (bottom row) NCAR-CAM5.3 clouds-off experiment (black contours, 10 m/s intervals) and in the shading the difference in wind between the (first column) all clouds-on, (second column) tropical clouds-on, and (third column) extratropical clouds-on and clouds-off experiments. The contour interval is 1 m/s for the shading, centered about 0, as in Figure 1. The rightmost column shows the difference in zonal mean zonal wind at 850 hPa between clouds-on and clouds-off for each experiment.

Although it is not possible to perform such an experiment with all of the COOKIE models, the differing impacts of cloud radiative effects in the tropics versus extratropics are captured as follows. The tropical impact is measured by the change in strength of the Hadley cell $\Delta\psi$. The extratropical impact is measured by the second derivative of the ACRE near the position of the eddy-driven jet (ACRE$_{\phi\phi}$, see section 2). Figure 3 shows the ACRE for the clouds-on simulation of each COOKIE model and marks the latitudes of the eddy-driven jet for each simulation. For the models for which data are available, the ACRE for the clouds-off simulations is plotted as well. Although there is general agreement that clouds act to heat the atmospheric column in the tropics and cool in the high latitudes and that there is a local maximum in ACRE in the midlatitudes, there are significant differences in the amplitude and detailed structure of ACRE between the models. In particular, the meridional gradient in ACRE near the latitude of the eddy-driven jet, which will impact the baroclinicity of the atmosphere and hence the preferred region for eddy growth and the latitude of the eddy-driven jet, varies strongly between models. Finally, note that outside of the tropics the ACRE in the clouds-off experiments is generally quite similar to the ACRE in the clouds-on experiment. This indicates that in the extratropics, the feedback of dynamical changes resulting from the inclusion of cloud radiative effects back onto the ACRE is relatively small.

To demonstrate the connection between changes in the strength of the Hadley cell, ACRE$_{\phi\phi}$ and the resulting eddy-driven jet shift, Figure 4 shows scatterplots between these quantities. Across the eight COOKIE simulations, and the additional eight customized experiments with the GFDL-AM2.1 and NCAR-CAM5.3 models (see supporting information), there is a clear connection between the change in Hadley cell strength $\Delta\psi$ and the jet shift $\Delta\phi$ ($r = -0.65$; Figure 4a). Although the connection between ACRE$_{\phi\phi}$ and $\Delta\phi$ is not as strong ($r = -0.41$; Figure 4b), it still explains an important part of the variance in the eddy-driven jet shift. For example, focusing on three models with similar positive changes in Hadley cell strength: CNRM-CM5.1, MPI-ECHAM6, and HadGEM2-A, their differing ACRE$_{\phi\phi}$ (see Figure 4b or Table 1) can at least partially explain their substantially varying responses to the imposition of cloud radiative effects (i.e., a strong equatorward shift, a weak equatorward shift, and a weak poleward shift, respectively). Using a different value of α, which is the latitude range over which ACRE is averaged when computing ACRE$_{\phi\phi}$, leads to moderate changes in the correlation computed for Figure 4b (e.g., $\alpha = 2°$ gives
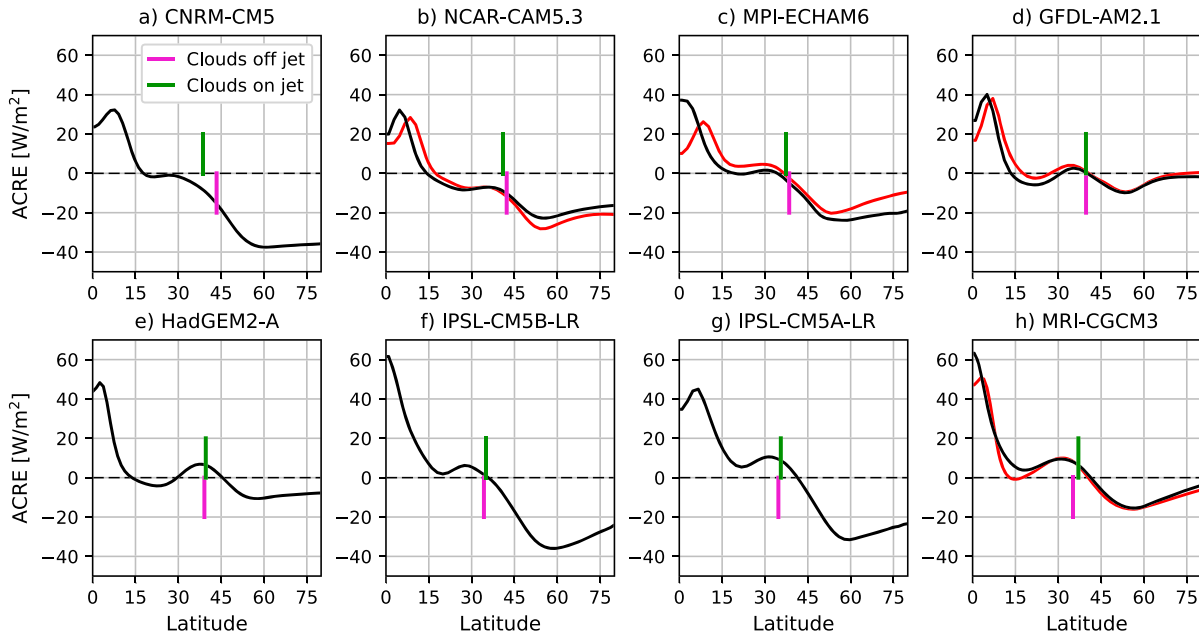
Figure 3. ACRE for the clouds-on simulations of each model, with the latitude of the eddy-driven jet in the clouds-off and clouds-on simulations marked by vertical magenta and green lines, respectively. The ACRE for the clouds-off simulation (computed only for diagnostic purposes) is shown in red, for the models for which it is available.

$r = -0.46$, $\alpha = 10°$ gives $r = -0.31$). In order to demonstrate the joint effects of $\Delta\psi$ and $ACRE_{\phi\phi}$ onto the jet shift, Figure 4c shows a scatterplot of these two quantities, with the color and size of the markers representing the sign and magnitude of $\Delta\phi$. Due to the negative correlations between each of these quantities and the jet shift, it is expected that points that fall in the upper right quadrant will have equatorward shifts, while those in the lower left quadrant will have poleward shifts. To quantify these connections, a least squares best fit of the function

$$\Delta\phi = A \cdot \Delta\psi + B \cdot ACRE_{\phi\phi} + C \qquad (4)$$

is made to the data. This plane, using the best fit computed values of $A = -0.046°/(10^9 \text{ kg/s})$, $B = -0.44°/(\text{W/m}^2)$, and $C = 0.04°$, is shown in Figure 4c. Using this linear regression, the separate impacts of $\Delta\psi$ and
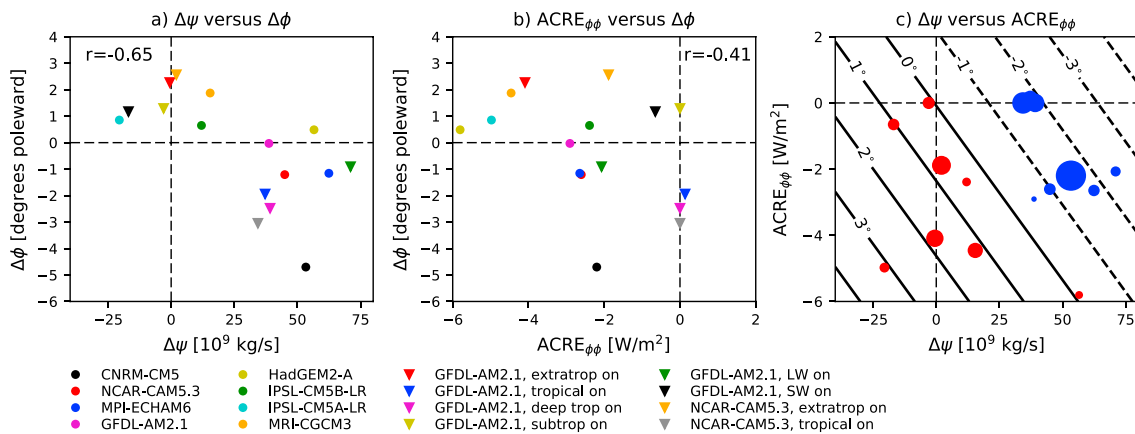

Figure 4. Scatterplots of (a) $\Delta\psi$ versus $\Delta\phi$, (b) $ACRE_{\phi\phi}$ versus $\Delta\phi$, and (c) $\Delta\psi$ versus $ACRE_{\phi\phi}$, with the size of markers representing the magnitude of $\Delta\phi$ (red poleward, blue equatorward). In Figure 4c, the least squares fit of equation (3) to the given data (including all the COOKIE simulations, and the additional GFDL-AM2.1 and NCAR-CAM5.3 experiments) is shown in the solid and dashed contours. Circle markers represent standard COOKIE experiments, while triangles indicate experiments where cloud radiative effects are only imposed in certain regions or for just longwave or shortwave.

ACRE$_{\phi\phi}$ can be removed from the data (Figures S5a and S5b) and the actual jet shift can be plotted against the predicted jet shift using equation (3) (Figure S5c). Together, the two variables explain 58% of the variance of the eddy-driven jet shift.

Figure S5c also makes it clear that there are two models whose behavior is furthest from the simple linear relationship: the actual jet shift for both the CNRM-CM5 and IPSL-CM5A-LR models is significantly more equatorward than the predicted shifts. For the CNRM-CM5 model, this may be because the climatological Hadley cell for the clouds-off simulation is the weakest out of all of the considered models and its eddy-driven jet in the clouds-off simulation is the most poleward. Previous research suggests that the eddy-driven jet position is more sensitive to the subtropical jet strength when it is further poleward and the subtropical jet is weaker (see Figure 3 of Ceppi et al., 2013). This connection is supported by the fact that there is a negative relationship between ϕ_{off} and $\Delta\phi$ ($r = -0.82$, computed across the eight standard COOKIE experiments listed in Table 1). It also results in the eddy driven jet latitude being more similar across models for the clouds-on experiments (standard deviation of 2.0°) than for the clouds-off experiments (standard deviation of 3.2°). For the IPSL-CM5A-LR model, despite a slight weakening in the strength of the Hadley cell as measured by the maximum of the stream function, there is not a clear weakening of the subtropical jet (Figure 1g), and this may explain the more moderate poleward shift of the eddy-driven jet than expected from the linear regression.

4. Conclusions and Discussion

Atmospheric general circulation models exhibit a wide range of responses of the position of their eddy-driven jet to the inclusion of cloud radiative effects. By separately imposing cloud radiative effects only in the tropics or in the extratropics, it was shown that clouds in each of these regions have opposing impacts on the position of the jet. In the tropics, high clouds warm the upper troposphere in the tropics and consequently accelerate the Hadley cell and thus the subtropical jet. A strengthened subtropical jet tends to lead to an equatorward shifted eddy-driven jet. However, cloud radiative effects in the extratropics also locally affect zonal mean temperature gradients and act to shift the position of the eddy-driven jet. It is found that clouds have a tendency to increase the temperature gradient on the poleward side of the eddy-driven jet, and hence, locally, they act to shift the jet poleward. Ultimately, the change in Hadley cell strength and the local impact of cloud radiative effects together are found to explain 58% of the variance across models of the meridional shift of the eddy driven jet. Interestingly, it is found that the latitude of the eddy-driven jet is much more consistent across models when cloud radiative effects are included.

Previous studies that have used the COOKIE framework to examine the impact of atmospheric cloud radiative effects onto the general circulation have primarily focused on the tropical circulation. However, Li et al. (2015) did find a weak equatorward shift of the eddy-driven jet (cf. their Figures 1a and 5b) in a model simulation that included topography. But given that different atmospheric GCMs, even in a simplified aquaplanet configuration, do not agree on the sign of the eddy-driven jet latitude response to the inclusion of atmospheric cloud radiative effects, it is necessary to treat with caution results examining the coupling between clouds and the extratropical circulation in only one or two models. Furthermore, because of the strong influence of the tropical circulation onto the extratropics, when examining the possible coupling between cloud radiative effects and circulation in the middle to high latitudes, it is necessary to consider the possible effects that cloud radiative effects in the tropics are having onto the higher latitudes.

Important questions for future work include addressing more precisely why the atmospheric cloud radiative effect is different across models, and why the Hadley cell response differs so strongly between models. To properly address this, the height-dependent cloud heating rates are needed, which are not standard output for COOKIE or CMIP5 (Taylor et al., 2012) experiments. Furthermore, other aspects of the simulations beyond the direct cloud heating could affect the changes in Hadley cell strength, such as the convection scheme or other parameterized processes, or the impacts of tropical variability onto the Hadley circulation. For the extratropics, it is evident from this study that subtle changes in the precise region of cloud heating (and more directly, ACRE gradients) will affect the position of the eddy-driven jet. Furthermore, in the extratropics there are large differences in the cloud heating rates between the boundary layer and the free troposphere (Figure S3), and the differing impacts of heating in each of these regions of forcing may be important for understanding the response of the eddy-driven jet.

This study has focused on specified-SST simulations, which necessarily limit to some extent the response of low clouds to changes in circulation. However, previous studies have emphasized the importance of low cloud changes modifying baroclinicity and hence the eddy-driven jet position (e.g., Ceppi et al., 2012). Although applying the COOKIE framework in a model with a slab or dynamical ocean is challenging due to the net surface cooling effect of clouds, possible future ways to address this issue would be to apply SST perturbations in a specified-SST model that mimic the low cloud radiative effect (as in Voigt & Shaw, 2016) or to include a Q-flux term or change the surface albedo such that a clouds-off slab ocean simulation would maintain the same globally averaged surface temperature as a clouds-on one, enabling a more realistic comparison. Finally, future work will also aim to use this study's novel understanding of the local and remote impacts of cloud radiative effects in order to better constrain the spread of eddy-driven jet responses to global warming across models.

References

Anderson, J., Balaji, V., Broccoli, A. J., Cooke, W. F., Delworth, T. L., Dixon, K. W., … Wyman, B. L. (2004). The New GFDL Global Atmospheric and Land Model AM2-LM2: Evaluation with prescribed SST simulations. *Journal of Climate*, 17, 4641–4673. https://doi.org/10.1175/JCLI-3223.1

Barnes, E. A., & Hartmann, D. L. (2010). Testing a theory for the effect of latitude on the persistence of eddy-driven jets using CMIP3 simulations. *Geophysical Research Letters*, 37, L15801. https://doi.org/10.1029/2010GL044144

Barnes, E. A., & Hartmann, D. L. (2011). Rossby wave scales, propagation, and the variability of eddy-driven jets. *Journal of the Atmospheric Sciences*, 68, 2893–2908. https://doi.org/10.1175/JAS-D-11-039.1

Bony, S., Stevens, B., Frierson, D. M. W., Jakob, C., Kageyama, M., Pincus, R., … Webb, M. J. (2015). Clouds, circulation and climate sensitivity. *Nature Geoscience*, 8, 261–268. https://doi.org/10.1038/NGEO2398

Bracegirdle, T. J., Shuckburgh, E., Sallee, J.-B., Wang, Z., Meijers, A. J. S., Bruneau, N., … Wilcox, L. J. (2013). Assessment of surface winds over the Atlantics, Indian, and Pacific Ocean sectors of the Southern Ocean in CMIP5 models: Historical bias, forcing response, and state dependence. *Journal of Geophysical Research: Atmospheres*, 118, 547–562. https://doi.org/10.1002/jgrd.50153

Brayshaw, D. J., Hoskins, B., & Blackburn, M. (2008). The storm-track response to idealized SST perturbations in an aquaplanet GCM. *Journal of the Atmospheric Sciences*, 65, 2842–2860. https://doi.org/10.1175/2008JAS2657.1

Ceppi, P., & Hartmann, D. L. (2015). Connections between clouds, radiation, and midlatitude dynamics: A review. *Current Climate Change Reports*, 1, 94. https://doi.org/10.1007/s40641-015-0010-x

Ceppi, P., & Hartmann, D. L. (2016). Clouds and the atmospheric response to warming. *Journal of Climate*, 29, 783–799. https://doi.org/10.1175/JCLI-D-15-0394.1

Ceppi, P., Hwang, Y.-T., Frierson, D. M. W., & Hartmann, D. L. (2012). Southern Hemisphere jet latitude biases in CMIP5 models linked to shortwave cloud forcing. *Geophysical Research Letters*, 39, L19708. https://doi.org/10.1029/2012GL053115

Ceppi, P., Hwang, Y.-T., Liu, X., Frierson, D. M. W., & Hartmann, D. L. (2013). The relationship between the ITCZ and the Southern Hemispheric eddy-driven jet. *Journal of Geophysical Research: Atmospheres*, 118, 5136–5146. https://doi.org/10.1002/jgrd.50461

Collins, W., Bellouin, N., Doutriaux-Boucher, M., Gedney, N., Hinton, T., Jones, C. D., …, Kim, J. (2008). Evaluation of HadGEM2 model, Met Office Hadley Centre Tech. Note 74, 47 pp.

Crueger, T., & Stevens, B. (2015). The effect of atmospheric radiative heating by clouds on the Madden-Julian Oscillation. *Journal of Advances in Modeling Earth Systems*, 7, 854–864. https://doi.org/10.1002/2015MS000434

Dufresne, J. L., Foujols, M.-A., Denvil, S., Caubel, A., Marti, O., Aumont, O., … Vuichard, N. (2013). Climate change projections using the IPSL-CM5 Earth System Model: From CMIP3 to CMIP5. *Climate Dynamics*, 40, 2123–2165. https://doi.org/10.1007/s00382-012-1636-1

Grise, K. M., & Medeiros, B. (2016). Understanding the varied influence of mid-latitude jet position on clouds and cloud-radiative effects in observations and global climate models. *Journal of Climate*, 29, 9005–9025. https://doi.org/10.1175/JCLI-D-16-0295.1

Grise, K. M., & Polvani, L. M. (2014). Southern Hemisphere cloud-dynamics biases in CMIP5 models and their implications for climate projections. *Journal of Climate*, 27, 6074–6092. https://doi.org/10.1175/JCLI-D-14-00113.1

Harrop, B. E., & Hartmann, D. L. (2016). The role of cloud radiative heating in determining the location of the ITCZ in aquaplanet simulations. *Journal of Climate*, 29, 2741–2763. https://doi.org/10.1175/JCLI-D-15-0521.1

Hourdin, F., Foujols, M.-A., Codron, F., Guemas, V., Dufresne, J.-L., Bony, S., … Bopp, L. (2013). Impact of the LMDZ atmospheric grid configuration on the climate and sensitivity of the IPSL-CM5A coupled model. *Climate Dynamics*, 40, 2167–2192. https://doi.org/10.1007/s00382-012-1411-3

Hourdin, F., Grandpeix, J.-Y., Rio, C., Bony, S., Jam, A., Cheruy, F., … Roehrig, R. (2013). The atmospheric component of the IPSL climate model with revisited parameterizations for clouds and convection. *Climate Dynamics*, 40, 2193–2222. https://doi.org/10.1007/s00382-012-1343-y

Hwang, Y.-T., & Frierson, D. M. W. (2013). Link between the double-Intertropical Convergence Zone problem and cloud biases over the Southern Ocean. *Proceedings of the National Academy of Sciences of the United States of America*, 110, 4935–4940. https://doi.org/10.1073/pnas.1213302110

Kang, S., & Polvani, L. M. (2011). The interannual relationship between the latitude of the eddy-driven jet and the edge of the Hadley cell. *Journal of Climate*, 24, 563–568. https://doi.org/10.1175/2010JCLI4077.1

Kidston, J., & Gerber, E. P. (2010). Intermodel variability of the poleward shift of the austral jet stream in the CMIP3 integrations linked to biases in 20th century climatology. *Geophysical Research Letters*, 37, L09708. https://doi.org/10.1029/2010GL042873

Lee, S., & Kim, H.-K. (2003). The dynamical relationship between subtropical and eddy-driven jets. *Journal of the Atmospheric Sciences*, 60, 1490–1503. https://doi.org/10.1175/1520-0469(2003)060<1490:TDRBSA>2.0.CO;2

Li, Y., & Thompson, D. W. J. (2016). Observed signatures of the barotropic and baroclinic annular modes in cloud vertical structure and cloud radiative effects. *Journal of Climate*, 29, 4723–4740. https://doi.org/10.1175/JCLI-D-15-0692.1

Li, Y., Thompson, D. W. J., & Bony, S. (2015). The influence of atmospheric cloud radiative effects on the large-scale atmospheric circulation. *Journal of Climate*, 28, 7263–7278. https://doi.org/10.1175/JCLI-D-14-00825.1

Li, Y., Thompson, D. W. J., Huang, Y., & Zhang, M. (2014). Observed linkages between the northern annular mode/North Atlantic Oscillation, cloud incidence, and cloud radiative forcing. *Geophysical Research Letters*, 41, 1681–1688. https://doi.org/10.1002/2013GL059113

Lindzen, R. S., & Farrell, B. (1980). A simple approximate result for the maximum growth rate of baroclinic instabilities. *Journal of the Atmospheric Sciences*, *37*, 1648–1654. https://doi.org/10.1175/1520-0469(1980)037<1648:ASARFT>2.0.CO;2

Medeiros, B., Williamson, D. L., & Olson, J. G. (2016). Reference aquaplanet climate in the Community Atmosphere Model, version 5. *Journal of Advances in Modeling Earth Systems*, *8*, 406–424. https://doi.org/10.1002/2015MS000593

Neale, R. B., & Hoskins, B. J. (2000). A standard test for AGCMs including their physical parameterizations: I: The proposal. *Atmospheric Science Letters*, *1*, 101–107. https://doi.org/10.1006/asle.2000.0022

Rädel, G., Mauritsen, T., Stevens, B., Dommenget, D., Matei, D., Bellomo, K., & Clement, A. (2016). Amplification of El Niño by cloud longwave coupling to atmospheric circulation. *Nature Geoscience*, *9*, 106–110. https://doi.org/10.1038/NGEO2630

Ramanathan, V., Cess, R. D., Harrison, E. F., Minnis, P., Barkstrom, B. R., Ahmad, E., & Hartmann, D. (1989). Cloud-radiative forcing and climate: Results from the Earth radiation budget experiment. *Science*, *243*, 57–63. https://doi.org/10.1126/science.243.4887.57

Shaw, T. A., Baldwin, M., Barnes, E. A., Caballero, R., Garfinkel, C. I., Hwang, Y.-T., … Voigt, A. (2016). Storm track processes and the opposing influences of climate change. *Nature Geoscience*, *9*, 656–665. https://doi.org/10.1038/NGEO2783

Simpson, I. R., & Polvani, L. M. (2016). Revisiting the relationship between jet position, forced response, and annular mode variability in the southern midlatitudes. *Geophysical Research Letters*, *43*, 2896–2903. https://doi.org/10.1002/2016GL067989

Slingo, A., & Slingo, J. M. (1988). The response of a general circulation model to cloud longwave radiative forcing. I: Introduction and initial experiments. *Quarterly Journal of the Royal Meteorological Society*, *114*, 1027–1062. https://doi.org/10.1002/qj.49711448209

Slingo, J. M., & Slingo, A. (1991). The response of a general circulation model to cloud longwave radiative forcing. II: Further studies. *Quarterly Journal of the Royal Meteorological Society*, *117*, 333–364. https://doi.org/10.1002/qj.49711749805

Stevens, B., Giorgetta, M., Esch, M., Mauritsen, T., Crueger, T., Rast, S., … Roeckner, E. (2013). Atmospheric component of the MPI-M Earth system model: ECHAM6. *Journal of Advances in Modeling Earth Systems*, *5*, 146–172. https://doi.org/10.1002/jame.20015

Stevens, B., Bony, S., & Webb, M. J. (2012). Clouds On-Off Klimate Intercomparison Experiment (COOKIE). Retrieved from: http://hdl.handle.net/11858/00-001M-0000-0024-580A-3

Taylor, K. E., Stouffer, R. J., & Meehl, G. A. (2012). An overview of CMIP5 and the experiment design. *Bulletin of the American Meteorological Society*, *93*, 485–498. https://doi.org/10.1175/BAMS-D-11-00094.1

Tselioudis, G., Lipat, B. R., Konsta, D., Grise, K. M., & Polvani, L. M. (2016). Midlatitude cloud shifts, their primary link to the Hadley cell, and their diverse radiative effects. *Geophysical Research Letters*, *43*, 4594–4601. https://doi.org/10.1002/2016GL068242

Voigt, A., & Shaw, T. A. (2015). Circulation response to warming shaped by radiative changes of clouds and water vapour. *Nature Geoscience*, *8*, 102–106. https://doi.org/10.1038/NGEO2345

Voigt, A., & Shaw, T. A. (2016). Impact of regional atmospheric cloud radiative changes on shifts of the extratropical jet stream in response to global warming. *Journal of Climate*, *29*, 8399–8421. https://doi.org/10.1175/JCLI-D-16-0140.1

Voldoire, A., Sanchez-Gomez, E., Salas y Mélia, D., Decharme, B., Cassou, C., Sénési, S., … Chauvin, F. (2013). The CNRM-CM5.1 global climate model: Description and basic evaluation. *Climate Dynamics*, *40*, 2091–2121. https://doi.org/10.1007/s00382-011-1259-y

Yukimoto, S., Adachi, Y., Hosaka, M., Sakami, T., Yoshimura, H., Hirabara, M., … Kitoh, A. (2012). A new global climate model of the Meteorological Research Institute: MRI-CGCM3: Model description and basic performance. *Journal of the Meteorological Society of Japan*, *90A*, 23–64. https://doi.org/10.2151/jmsj.2012-A02